

A Review of Recent Developments in Estuarine Scalar Flux Estimation

D. A. JAY^{1,2}

*Center for Coastal and Land-Margin Research
Oregon Graduate Institute
P.O. Box 91000
Portland, Oregon 97291-1000*

R. J. UNCLES²

*Plymouth Marine Laboratory
Plymouth PL1 3DH
United Kingdom*

J. LARGIER²

*Coastal Studies
Scripps Institute of Oceanography
La Jolla, California 92093*

W. R. GEYER²

*Ocean Engineering Department
Woods Hole Oceanographic Institution
Woods Hole, Massachusetts 02543*

J. VALLINO²

*Ecosystems Studies
Marine Biological Laboratory
Woods Hole, Massachusetts 02543*

W. R. BOYNTON²

*Chesapeake Biological Laboratory
University of Maryland
Solomons, Maryland 20688-0038*

ABSTRACT: The purpose of this contribution is to review recent developments in calculation of estuarine scalar fluxes, to suggest avenues for future improvement, and to place the idea of flux calculation in a broader physical and biogeochemical context. A scalar flux through an estuarine cross section is the product of normal velocity and scalar concentration, sectionally integrated and tidally averaged. These may vary on interannual, seasonal, tidal monthly, and event time scales. Formulation of scalar fluxes in terms of an integral scalar conservation expression shows that they may be determined either through "direct" means (measurement of velocity and concentration) or by "indirect" inference (from changes in scalar inventory and source/sink terms). Direct determination of net flux at a cross section has a long and generally discouraging history in estuarine oceanography. It has proven difficult to extract statistically significant net (tidally averaged) fluxes from much larger flood and ebb transports, and the best mathematical representation of flux mechanisms is unclear. Observations further suggest that both lateral and vertical variations in scalar transport through estuarine cross sections are large, while estuarine circulation theory has focused on two-dimensional analyses that treat either vertical or lateral variations but not both. Indirect estimates of net fluxes by determination of the other relevant terms in an integral scalar conservation balance may be the best means of determining scalar import-export in systems with residence times long relative to periods of tidal monthly fluctuations. But this method offers little insight into the interaction of circulation modes and scalar fluxes, little help in verifying predictive models, and may also be difficult to apply in some circumstances. Thus, the need to understand, measure, and predict anthropogenic influences on transport of carbon, nutrients, suspended matter, trace metals, and other substances across the land-margin brings a renewed urgency to the issue of how to best carry out estuarine scalar flux determination. An interdisciplinary experiment is suggested to test present understanding, available instruments, and numerical models.

Introduction

The purpose of this contribution is to review recent developments in calculation of estuarine scalar fluxes, to suggest avenues for future improvement, and to place the idea of flux calculation in a broader physical and biogeochemical context. The impetus for such a review comes from the Land Margin Ecosystem Research (LMER) program funded by the United States National Science Foundation. LMER is designed to address urgent

problems caused by anthropogenic and climate change in coastal zones. Six sites have been studied during the 1989-1995 period: Chesapeake Bay, Tomales Bay, Waquoit Bay, the Columbia River estuary, Plum Island Sound, and the Georgia rivers (Table 1). LMER studies in Tomales and Waquoit bays (now complete) focused broadly on nutrient geochemistry. After an initial nutrient geochemistry phase, studies in Chesapeake Bay have been expanded to examine human impacts on the estuarine food chain as a whole. The Columbia River program concentrates on the ecosystem role of particles and the Plum Island Sound group has emphasized the influence of carbon sources on food

¹ Corresponding author. Tele: 503/690-1372; Fax: 503/690-1273; Email: djay@ese.ogi.edu.

² LMER Scalar Transport Working Group.

TABLE 1. Comparative aspects of LMER sites.^a

	Chesapeake Bay	Tomales Bay	Waquoit Bay	Columbia River	Plum Island Sound	Satilla River
Estuary area, km ²	11,478	28	6.3	420	7.2-14.9	68-257
Mean depth, m	9	3.1	0.9	10	2.3	3.5
Mean tidal range, m	0.5	1	0.7	1.7	2.6	2
Tidal prism, 10 ⁶ m ³	1,720	28	4.4	680	28.7	470-570
Watershed area, 10 ³ km ²	164	0.57	0.046	660.5	0.58	9.14
Watershed max elevation, m	1,220	794	100	3,500	100	76
Mean river flow, 10 ⁶ m ³ d ⁻¹	190	0.4	0	630	0.88	6
Groundwater flow, 10 ⁶ m ³ d ⁻¹	10	0.015	0.115	20	NA	NA
Sewage discharge, 10 ⁶ m ³ d ⁻¹	5.4	0	0	1	NA	NA
Precipitation, 10 ⁶ m ³ d ⁻¹	31	0.076	0.021	1,722	0.030	NA
Evaporation, 10 ⁶ m ³ d ⁻¹	14,900	39.2	11.3	294	0.013	NA
Freshwater inflow/tidal prism	0.066	0.008	0.015	0.49	0.015	NA
Salinity range, PSU	0-30	0-38	0-32	0-33	0-33	0-35
Temperature range, °C	-1-30	5-23	1-20	0-23	-1-23	5-30
Sediment input, 10 ⁶ mt yr ⁻¹	5.5	0.3	0.02	2.3	0.004	NA
Sedimentation rate, mm yr ⁻¹	2-15	1	2	5	NA	NA
Range of SPM, mg l ⁻¹	5-300	0-200	NA	1-1,000	NA	50-20,000

^a Modified from LMER Coordinating Committee (1992).

web structure. The Georgia Rivers program compares five river estuaries and considers both particle and ecosystem structure problems. Specific questions addressed by these projects are described by the LMER Coordinating Committee (1992), but answers to many of these imply an ability to calculate horizontal fluxes.

The LMER study sites are quite diverse. Chesapeake Bay is a classic coastal-plain estuary, Tomales Bay is a bar-built embayment within a drowned rift valley, Waquoit Bay is a small lagoon, and Plum Island Sound is bar-built embayment with more fluvial forcing than Waquoit or Tomales bays. The remaining systems are river estuaries. The Columbia River drains one of the largest basins in North America; this basin has considerable mountainous and glaciated terrain, nonetheless, it is relatively impoverished in terms of fine sediment input. The Georgia river estuaries are of two basic types: tannic, "blackwater" systems draining the coastal plain only, and piedmont systems with larger basins and greater river inflow. Chesapeake Bay, and the Columbia and Satilla river estuaries (the latter a Georgia blackwater system) trap particles in turbidity maxima. The Satilla is more turbid than either the Chesapeake or the Columbia and accumulates liquid mud near the upstream limits of salinity intrusion.

The scalar fluxes of interest here are horizontal. Thus, a scalar flux through a cross section is a product of a horizontal, normal velocity and a scalar variable being advected by the flow, this product being integrated over an appropriate time interval such as a tidal cycle. Estimation of cross-sectional scalar fluxes as an aspect of scalar conservation has engaged the interest of estuarine

scientists for more than three decades. As difficult as flux measurements have proven to be, their direct or indirect (as defined in the next section) inference is vital for several reasons: (1) Flux estimation is essential to calculation of residence time, T_R , a parameter essential to understanding and classifying estuaries and their ecosystems. (2) It is vital to comprehend the mechanisms that generate tidal-average fluxes, because these residual transports are the engine for long-term effects of ecological, social, and geological importance. An ability to predict long-term changes in fluxes must be based on knowledge of flux mechanisms, and their role in and response to estuarine circulation. (3) Net fluxes of nutrients, carbon, and total suspended particulate matter (SPM) must be measured, predicted, and understood to quantify the global consequences of anthropogenic change in the land margin and their effects on fluxes of ecologically relevant substances including pollutants. (4) Scalar fluxes are increasingly relevant in other contexts. Analyses of the origin of some sedimentary rocks and of the geological evolution of estuaries require, for example, an understanding of fluxes of sediment and organic matter into and out of estuaries and coastal seas over very long time scales. This contribution focuses on methodology for and future applications of flux estimation, rather than cataloging past studies already reviewed by Dyer (1973) and Jay (1991).

There are several reasons to re-think estuarine flux estimation methods. One is an obvious mismatch between a need (expressed, for example, in the LMER program) to determine scalar fluxes from coastal systems to the ocean on an annual to decadal basis and a generally discouraging history of attempts to calculate net fluxes from observa-

tions. Another is that recent developments in instrument technology, numerical modeling, and theory suggest several possible methods to minimize the gap between desired results and available flux calculation methods. There is also a need to understand the relationship between estuarine time scales as set by T_R and the flux calculation method most appropriate to the system. Finally, characterization of fluxes has considerable potential, not yet realized, as a comparative tool. The following discussion will review developments or suggest new approaches in each area.

Estimation and interpretation of scalar fluxes is an interdisciplinary research challenge. Given an estuarine morphology, the velocity field is generally controlled by physical processes, tidal propagation, winds, and freshwater discharge. Biological and biogeochemical processes may, however, set bottom roughness that in part determines the velocity profile, and on longer time scales, contribute to the evolution of channel morphology. The scalar quantity in a flux calculation may be entirely determined by physical processes (as for salt), but the scalars of greatest interest and difficulty are those associated with the biosphere, whose distributions are determined by both advection and the distributions of sources and sinks, for example, SPM, nutrients, pollutants, and plankton.

Flux Formulations

MASS CONSERVATION

Estimation of estuarine cross-sectional fluxes is an application of mass conservation for the scalar of interest. An integrated scalar conservation equation may be written:

$$\frac{\partial}{\partial t} \int_{x_1}^{x_2} \int \bar{C} d\bar{A} dx = - \int \overline{UC} d\bar{A} \Big|_{x_1}^{x_2} + \int \bar{B} dS + \int_{x_1}^{x_2} \int \bar{\Gamma} dA dx \quad (1)$$

where:

x , y , and z are the along-channel, across-channel and vertical coordinates,

t is time

C is scalar concentration

U is along-channel velocity

an overbar — indicates a tidal-cycle average, $d\bar{A} = dydz$ is the tidal-cycle average area of the estuarine cross section,

$dS = dydx$ is the area of the seabed and/or free surface between x_1 and x_2 ,

B is a source or sink term at the sea surface or seabed,

and Γ is an internal source or sink.

The left-hand (l.h.) side of Eq. (1) is the rate of change of tidal-average concentration \bar{C} of scalar quantity C in a tidal-average volume extending in the along-channel (x) direction from x_1 to x_2 . The right-hand (r.h.) side consists of two types of terms. The first is a tidal average of divergence of the horizontal flux of C . The remaining two are the bed and/or surface and internal source and/or sink terms of C . The bed-surface term encompasses particulate settling and erosion at the seabed, seabed groundwater source or loss terms for dissolved scalars, and air-sea exchange. The final term may include the results of biological activity, and for individual size classes of SPM, the results of aggregation or disaggregation.

Estuarine studies typically place x_2 at the upstream limit of salinity intrusion (x_L) where the salt flux vanishes. The l.h. side of Eq. (1) then represents the time change of the estuarine inventory $\int_{x_1}^{x_L} \bar{C} d\bar{A} dx$ of \bar{C} landward of x_1 . Salt is also conservative, eliminating the last two terms on the r.h. side. Thus, the time change in total estuarine salt content is determined solely by the net, nontidal flux through the section at x_1 :

$$\frac{\partial}{\partial t} \int_{x_1}^{x_L} \int \bar{C} d\bar{A} dx = \int \overline{UC} d\bar{A} \Big|_{x_1} \quad (2)$$

Expressions (1) and (2) embody several assumptions: (a) a two-timing assumption that temporal variability occurs on two distinct time scales, intratidal and subtidal; (b) the ratio of tidal amplitude to mean depth is $\ll 1$ (a small-amplitude assumption); and (c) the momentum-conveying width is not temporally variable. Such an analysis is probably sufficient for the systems considered in the LMER program and many others as well. A more complex development is needed for macrotidal estuaries and wide, shallow systems where much of the scalar exchange occurs over tidal flats but no entirely satisfactory method is available.

The flux term on the r.h. side in Eq. (1) and Eq. (2) may be determined by "indirect" or "direct" methods. The most obvious indirect approach is evaluation of time changes in the estuarine inventory of \bar{C} [the l.h. side of Eq. (1) or Eq. (2)] and, for a nonconservative scalar, calculation of the relevant source and sink terms. If averaging over a sufficient time interval allows assumption of a steady state (i.e., that the l.h. side of Eq. (1) vanishes), a simpler approach may be possible; one may evaluate the fluxes on the r.h. side of Eq. (1) from the nonconservative term(s) alone (e.g., from burial in the sediment; Boynton et al. 1980). In systems with strong tides and short residence times, a steady state cannot be assumed and the estuarine inventory of a scalar of interest may be

difficult to determine on a synoptic basis. Fluxes must then be determined directly. The "direct" approach consists of calculation of the flux(es) on the r.h. side of Eq. (1) or Eq. (2) from observations of U and C . Alternatively, one may use observations of U and C to validate numerical models of the velocity and scalar fields and calculate the fluxes in Eq. (1) or Eq. (2) from model outputs.

DEFINITION OF TRANSPORT MODES

Forecasting anthropogenic effects requires understand transport processes generating fluxes. Considerable effort has been devoted to development of expansions of the r.h. side of Eq. (2) in terms of physical transport modes (reviewed by Dyer 1973 and Jay 1991). Arguably the simplest useful approach is to average U and C over the channel width and distinguish depth-average quantities and vertical deviations, leaving aside for the moment complications associated with lateral variability. Each variables may then be taken as the sum of a residual, low-frequency component and a small number ($j = 1, n$) of tidal species. Thus:

$$\begin{aligned} U(x, z, t) &= \langle \bar{U}(x) \rangle + \sum_{j=1}^n \langle U_j(x, t) \rangle \\ &\quad + \bar{U}_v(x, z) + \sum_{j=1}^n U_{jv}(x, z, t) \\ C(x, z, t) &= \langle \bar{C}(x) \rangle + \sum_{j=1}^n \langle C_j(x, t) \rangle \\ &\quad + \bar{C}_v(x, z) + \sum_{j=1}^n C_{jv}(x, z, t) \end{aligned} \quad (3)$$

where brackets $\langle \rangle$ indicate a depth average, and subscript v indicates a depth deviation from a depth-averaged quantity. Substitution of these definitions into Eq. (2) gives

$$\begin{aligned} \int \bar{UC} \, d\bar{A} &= \bar{A} \left(\langle \bar{U} \rangle \langle \bar{C} \rangle + \sum_{j=1}^n \langle \bar{U}_j \rangle \langle \bar{C}_j \rangle \right. \\ &\quad \left. + \langle \bar{U}_v \bar{C}_v \rangle + \sum_{j=1}^n \langle \bar{U}_{jv} \bar{C}_{jv} \rangle \right). \end{aligned} \quad (4)$$

The four terms on the r.h. side of Eq. (4) are commonly known as the mean, tidal, mean-shear, and tidal-shear advective transports, respectively. This formulation is very simple if all time variability is lumped into a single tidal mode, but observations discussed below show that SPM and salt interact differently with the tidal flow. Thus, the various tidal species should be distinguished if the scalar transport mechanisms are to be understood. The number of terms $[2(n + 1)]$ escalates as the number of species n increases. Inclusion of lateral vari-

ations in U and C would lead to $4(n + 1)$ terms on the r.h. side of Eq. (2).

Difficulties with various versions of the above expansion over the last several decades suggested to Jay (1991) that a different approach was needed. He simplified the r.h. side of Eq. (2) by distinguishing between river flow and Stokes drift and then, after use of Eq. (3), eliminated terms that should cancel one another. This approach leads to

$$\begin{aligned} \int \bar{UC} \, d\bar{A} &\cong -\bar{Q}^R \langle \bar{C} \rangle + \bar{A} \left(\langle \bar{U}_v \bar{C}_v \rangle + \sum_{j=1}^n \langle \bar{U}_{jv} \bar{C}_{jv} \rangle \right) \\ &\cong -\bar{Q}^R \langle \bar{C} \rangle + \bar{A} \langle \bar{U}_v^L \bar{C}_v \rangle \end{aligned} \quad (5)$$

where $-\bar{Q}^R$ is the integral (outward) river flow transport, and \bar{U}_v^L is the shear in the mean along-channel Lagrangian velocity. \bar{U}^L is a sum of an Eulerian mean along-channel velocity, \bar{U} , and a Stokes drift velocity, \bar{U}^S . This approach uses an equivalence of the Stokes transport of a mean scalar field and the tidal transport of tidal variations in this mean field (the Generalized Lagrangian Mean or GLM assumption), a relationship that is valid for small-amplitude tides in narrow tidal channels only (Andrews and McIntyre 1978; Middleton and Loder 1989). It further employs a very strong constraint implicit in two-dimensional channel geometry—the total Eulerian outflow is seaward and (for steady waves) is the sum of the outward riverflow and an Eulerian flow that exactly matches the landward Stokes drift; this is commonly called the Stokes drift compensation flow. Thus, the landward transport of $\langle \bar{C} \rangle$ by the vertically integrated Stokes drift $\langle \bar{U}_j^S \rangle$ due to constituent j should be exactly compensated by a seaward transport of $\langle \bar{C} \rangle$ by the Eulerian Stokes drift compensation flow associated with that constituent.

It is useful for calculation of T_R to integrate Eq. (5) in the along-channel direction and derive a relationship equivalent to Eq. (1) (Jay and Musiak 1994):

$$\begin{aligned} \frac{\partial}{\partial t} \int_{x_1}^{x_2} \bar{C} \, d\bar{A} \, dx &= \left[-\bar{Q}^R \langle \bar{C} \rangle + \bar{A} \left(\langle \bar{U}_v \bar{C}_v \rangle + \sum_{j=1}^n \langle \bar{U}_{jv} \bar{C}_{jv} \rangle \right) \right] \Big|_{x_1}^{x_2} \\ &\quad + \int \bar{B} \, dS + \int_{x_1}^{x_2} \bar{\Gamma} \, d\bar{A} \, dx \end{aligned} \quad (6)$$

T_R is calculated by dividing the inventory of C by the sum of the inward or outward fluxes, assuming a steady state. Equation (6) shows that a gain or loss of material between sections defined by x_1 and

x_2 can occur through: a) spatial convergence or divergence in river-flow transport or along-channel shear fluxes (products of velocity shear and scalar stratification) at residual and tidal frequencies, and/or b) input or loss of material via source and sink terms. Equation (6) contains only $n + 2$ horizontal transport terms because the integral tidal and mean advective terms have been eliminated.

Understanding how lateral variability affects the integral transport in Eq. (1) or Eq. (2) requires explicit inclusion of lateral variations in U and C :

$$\begin{aligned}\langle \bar{U} \rangle &= \langle \bar{U} \rangle + \langle \bar{U}_b \rangle & \langle U_j \rangle &= \langle \{U_j\} \rangle + \langle U_{jb} \rangle \\ \langle \bar{C} \rangle &= \langle \bar{C} \rangle + \langle \bar{C}_b \rangle & \langle C_j \rangle &= \langle \{C_j\} \rangle + \langle C_{jb} \rangle \\ \bar{U}_v &= \langle \bar{U}_v \rangle + \bar{U}_{vb} & U_{jv} &= \langle \{U_{jv}\} \rangle + U_{jvb} \\ \bar{C}_v &= \langle \bar{C}_v \rangle + \bar{C}_{vb} & C_{jv} &= \langle \{C_{jv}\} \rangle + C_{jvb}\end{aligned}\quad (7)$$

where $\{ \}$ represents a width average and the subscript b a lateral deviation from a width average. The expansion of Eq. (4) to include width variations in U and C leads to four vertically integrated and four vertical shear terms:

$$\begin{aligned}\int \bar{UC} \, d\bar{A} &= \bar{A} \left(\langle \{U\} \rangle \langle \{C\} \rangle + \langle \bar{U}_b \rangle \langle \bar{C}_b \rangle \right) \\ &+ \sum_{j=1}^n \langle \{U_j\} \rangle \langle \{C_j\} \rangle + \sum_{j=1}^n \langle \{U_{jb}\} \rangle \langle \{C_{jb}\} \rangle \\ &+ \bar{A} \left(\langle \{U_v\} \rangle \langle \{C_v\} \rangle + \langle \bar{U}_{vb} \rangle \langle \bar{C}_{vb} \rangle \right) \\ &+ \sum_{j=1}^n \langle \{U_{jv}\} \rangle \langle \{C_{jv}\} \rangle + \sum_{j=1}^n \langle \{U_{jvb}\} \rangle \langle \{C_{jvb}\} \rangle.\end{aligned}\quad (8)$$

The GLM approach used to derive Eq. (5) leads to

$$\begin{aligned}\int \bar{UC} \, d\bar{A} &= -\bar{Q}^R \langle \bar{C} \rangle + \bar{A} \left(\langle \bar{U}_v \rangle \langle \bar{C}_v \rangle + \sum_{j=1}^n \langle \bar{U}_{jv} \rangle \langle \bar{C}_{jv} \rangle \right) \\ &+ \langle \bar{U}_{vb} \rangle \langle \bar{C}_{vb} \rangle + \sum_{j=1}^n \langle \bar{U}_{jvb} \rangle \langle \bar{C}_{jvb} \rangle \\ &+ \langle \bar{U}_b \rangle \langle \bar{C}_b \rangle + \sum_{j=1}^n \langle \bar{U}_{jb} \rangle \langle \bar{C}_{jb} \rangle\end{aligned}\quad (9)$$

if width variations in U and C are considered. Each of the last six terms on the r.h. side of Eq. (9) may give either landward or seaward transport, but their sum must yield a net landward transport to counter the seaward transport by the riverflow in the first term on the r.h. side. We will refer to the

first four of the six terms in the parentheses on the r.h. side of Eq. (9) collectively as the mean and tidal components of vertical shear advection. The final two terms constitute the mean and tidal contributions to integral lateral shear advection. An equation analogous to Eq. (6) is a direct extension of Eq. (9).

It is worth summarizing the assumptions under which Eq. (1) to Eq. (9) were derived before considering their relationship to estuarine circulation theory. All assume steady, small-amplitude tides and a spectral separation between tidal and low-frequency processes; Eq. (5) and Eq. (9) further assume a channelized topography and apply only to narrow estuaries. None of the above theoretical expressions include tidal variations in width or scalar transport over intertidal areas, which might add terms to the r.h. side of Eq. (4), Eq. (5), and Eq. (9). Intertidal transport may be of little importance in a system with narrow tidal flats, but these fluxes may be quite important in maintaining salt and sediment balances in macrotidal systems. Some uses of Eq. (5) and Eq. (9) further require assumption of a steady scalar balance unless fluctuations in an estuarine scalar inventory can be measured.

Estuarine Flux Calculations— A Search for Meaning

FLUX CALCULATIONS AND CIRCULATION THEORY

The utility of the direct approach to future flux calculations is the primary subject of interest here. Before considering this issue, however, it is useful to place estuarine flux calculations in a historical context of wave flux estimation. A striking feature of the estuarine flux literature is its empirical quality. With the exception of the Hansen and Rattray (1966) classification scheme (extended by Rattray and Uncles 1983) and the analyses of Fischer (1976), little attempt has been made to connect estuarine circulation to the salt fluxes that must maintain it. The result has been a welter of confusing transport expansions filled with terms of uncertain meaning. The confusion has been worsened by persistent difficulties in obtaining statistically significant results. Determination of tidal-cycle average net flux as a small difference between large flood and ebb fluxes has proven particularly elusive. Errors limiting the accuracy of flux estimates may stem from inadequate resolution of small-scale velocity variability (Boon 1978; Kjerfve and Proehl 1979), imprecise knowledge of velocity and SPM near the bed (Smith 1977), and inadequate resolution of salinity gradients near fronts and the free surface (Uncles et al. 1985). Fluctuations in scalar inventory due (e.g., for salt) to

weather systems and river flow variations do not impair statistical validity, but they do complicate interpretation of results. Reduction of errors and uncertainty through improved sampling, better theoretical formulations, and more attention to the inventory side of Eq. (1) are all needed.

This isolation of circulation theory from analyses of scalar fluxes is in part a historical accident and in part a consequence of the inherent complexity of estuaries. Atmospheric science pursued a very different course between 1960 and 1980, with mean and wave fluxes being treated as an integral part of atmospheric circulation theory (Dunkerton 1981). Estuarine science can, potentially at least, now incorporate ideas from atmospheric science (Middleton and Loder 1989). The greatest difficulty in this regard lies perhaps with the discrepancies between observations of flux mechanisms and circulation theory. Available circulation theories for stratified estuaries from Hansen and Rattray (1965) to Jay and Musiak (1996) focus on the vertical dimensional and vertical shear advection. Analyses that include lateral circulation variability in stratified or estuarine systems (e.g., Kalkwijk and Booij 1986; Geyer 1993) do not as yet constitute a complete theory because they do not explain residual flow generation and scalar flux variability. The history of estuarine flux studies, including the observations discussed below, indicates the importance of lateral variations in scalar transport not included in any present theory.

The discrepancy between flux transport observations and two-dimensional (x - z) circulation theory can be understood in formal terms from Eq. (9). The first four terms inside the parenthesis on the r.h. side of Eq. (9) detail lateral variations in the vertical shear, stratification correlations terms [r.h. side of Eq. (5)] that result from lateral variations in vertical mixing and depth acting. The last two terms on the r.h. side of Eq. (9) represent net transport by lateral shear dispersion. This process has no analog in two-dimensional (x and z) theories that neglect lateral variability. The importance of these terms emphasizes the three-dimensionality of estuarine transport and clearly indicate why two-dimensional (x - z) theories cannot totally explain transport, even in narrow channelized estuaries. That is, the vertically averaged quantities that do appear in such theories ($\langle U \rangle$ and $\langle C \rangle$) cannot bring about any net transport [as per Eq. (5)], and the relevant vertically averaged terms ($\langle U_b \rangle$ and $\langle C_b \rangle$) are absent. These terms may be relatively small in some highly channelized systems, but they are of such dominant importance in broad, shallow basins with weak buoyancy forcing that existing theories for those systems (reviewed by Zimmerman 1986) have focused on vertically integrated

analyses and totally ignored the vertical shear correlation terms.

LATERAL VARIABILITY AND STATISTICAL SIGNIFICANCE

The earliest calculations that distinguished fluxes at tidal and residual frequencies and that included Stokes drift effects to achieve an approximate Lagrangian mean transport were those of Bowden (1963) and Hansen (1965). Numerous more detailed studies followed, as reviewed by Dyer (1973), Officer (1976), and Jay (1991). The prior flux calculations of interest here are those that attempted to resolve lateral variability and examined the statistical validity of calculated fluxes. The first such study was that of Boon (1978). He made detailed measurements of velocity and SPM at the mouth of a weakly stratified, 10.5 m wide tidal creek and analyzed errors in velocities and transport estimates. Because of its small size and absence of buoyancy effects, this marsh creek presented a minimum of complexity in the velocity field, and the resulting dataset represented what was at the time an upper limit on sample density. Nonetheless, the resulting nontidal water and sediment transport estimates were of marginal statistical significance. Statistical analyses of subsets of the data showed that errors of $\pm 7\%$ were likely in individual estimates of instantaneous cross-sectional flux, with probable errors of ± 7 - 10% in estimates of total flood and ebb water transports. Even though cross-sectional distributions of scalars in this vertically homogeneous tidal marsh creek were fairly simple, relative errors in scalar transports cannot be less than those for water transport. Thus, only a substantial net scalar transport could be detected, and such a transport is unusual in many systems.

Kjerfve and Proehl (1979) conducted a larger scale experiment in which water transport across the mouth of the 320 m wide entrance to North Inlet was measured over three tidal cycles using 10 stations across the section and 125 field workers. Despite the absence of dynamically significant stratification, channel curvature caused the velocity field to be considerable more complicated than the distributions of salinity and other scalars. Results were again of marginal statistical significance.

Stratified systems offer the likelihood that both scalar and velocity distributions may be quite complex, and this has frequently led to difficulties in achieving a reasonable salt balance (e.g., Dyer 1974; Murray and Siripong 1978; Dyer et al. 1992). Discrepancies between landward and seaward transport have in some cases been as large as a factor of three or four, but it is often unclear whether a failure to achieve balance is entirely the result of errors in measurements, or whether part

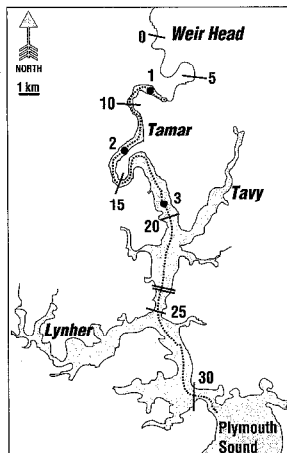


Fig. 1. Locations of sections 1, 2, and 3 (indicated by ●) in the Tamar estuary near Plymouth, England. Subdivision of the estuary into 5-km intervals is also shown.

of the apparent error is due to intratidal changes in estuarine salt content. Identifying the cause of the discrepancy would entail simultaneous flux calculations and monitoring of the estuarine scalar inventory [l.h. side of Eq. (1) or Eq. (2)], something that has not yet been attempted.

Estimates of water and salt transport at several sections of the Tamar estuary by Uncles et al. (1985) constitute an exception to the general trend of internally inconsistent transport results for stratified estuaries (Fig. 1). The success of this project emphasizes the necessity of resolving lateral variations in the velocity field. The cross sections used in this study were chosen to minimize lateral variability of tidal currents due to channel curvature. But, along-channel tidal currents still

showed strong lateral variability associated with the combined effects of stratification and lateral variations in depth (Fig. 2). The density-driven residual currents in the Tamar vary with channel depth; landward transport occurs primarily in the deepest part of the channel while outflow occurs along channel flanks (Fig. 3). This distribution of residual flow is mirrored in the salt transport field (Fig. 4), a phenomenon first noted by Fischer (1976).

SPM distributions may exhibit other complications; for example, lateral variability related to bed stress at the point of erosion rather than the point of measurement. Thus, in the Columbia River (Fig. 5), the high-velocity core in Fig. 6a is seen in the deepest part of cross section NCI whereas the SPM distribution seems to reflect bank erosion in shallow water landward of the measurement section (Fig. 6b). Further evidence for the influence of erosion remote from the measurement location can be seen in frequent above-bed SPM maxima coincident with an interfacial velocity maximum during periods of high stratification (Reed and Donovan 1994).

The generally frustrating history of estuarine scalar transports calculations has caused a shift in the emphasis over the last decade away from determination of net transport. Several recent analyses have employed alternative flux formulations and/or have used flux calculations primarily as a means to obtain dynamical insight (Lewis and Lewis 1983; Winterwerp 1983; Dronkers and van de Kreeke 1986; Jay and Smith 1990; West et al. 1990). Additional approaches and technologies are discussed below.

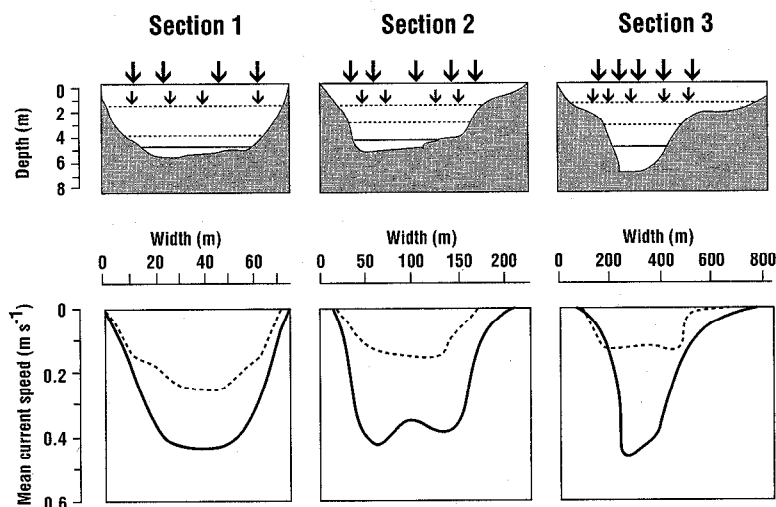


Fig. 2. Channel topography (top panel) for velocity and salinity sampling on sections 1, 2, and 3 in the Tamar estuary, high and low water lines for neap (---) and spring (—) tides are shown. The lateral profiles of mean, along-channel tidal speeds for neap (---) and spring (—) tides for each section are shown in the lower panel.

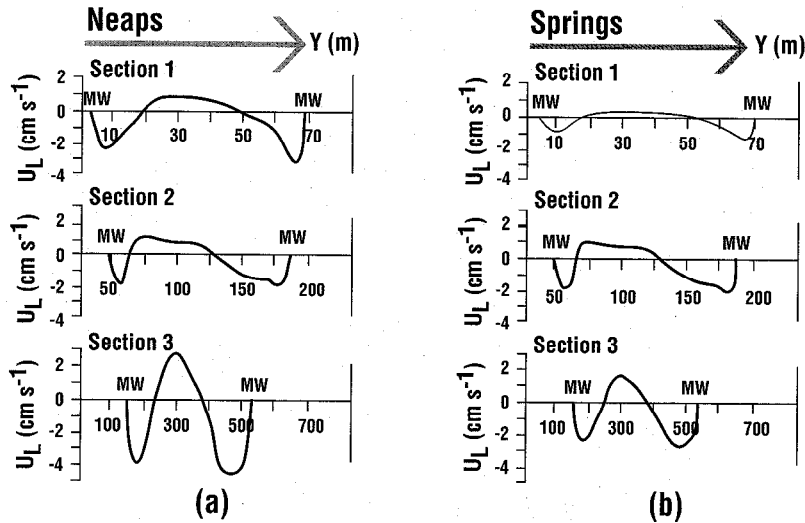


Fig. 3. Lateral variations in residual density-driven or gravitational circulation in the Tamar estuary. The water surface has been fixed at mean water level (MW) for these calculations. Negative values on the y-axis indicate down estuary movement.

Transport Processes, Residence Times, and Estuarine Comparison

SCALAR TRANSPORT AND THE CONCEPT OF RESIDENCE TIME

The role of salt fluxes in maintenance of estuarine stratification and the centrality of stratification in estuarine classification systems motivate use of flux estimates and transport processes to compare estuaries. The diversity of types amongst LMER study sites is formidable (Table 1), and they form only a small subset of North American estuaries. Table 2 describes the dominant salt flux mechanism, T_R , flushing character, and suggested flux calculation method for selected LMER estuaries. Substantial differences in scalar transport processes exist between LMER estuaries and from season-to-season within individual estuaries. Tidal monthly and shorter fluctuations in salt balance have been observed in the Columbia and Chesapeake, and are likely in the other systems.

Residence time, T_R , is a concept closely related to that of scalar fluxes because both are aspects of conservation of mass. T_R is the estuarine inventory of a particular scalar divided by the sum of fluxes into (or out of) the system on the r.h. side of Eq. (1) or Eq. (6), under the assumption that this inventory is invariant in time (i.e., that the l.h. side of these relations vanishes). T_R is not a property of a basin but of a particular scalar in a basin. If we wish to know T_R , there is no escape from direct or indirect estimation of fluxes. Salt and fresh water may behave differently in stratified systems, with silled fjords offering examples of extreme differences in T_R values for salt and water. Nonetheless T_R values for salt and fresh water are, for most es-

tuarine systems aside from fjords, usually similar and representative of the behavior of many other scalars.

Estimates of T_R in Table 2 are derived from Smith et al. (1991) for Tomales Bay, Neal (1972) for the Columbia River estuary, and other LMER observations. If a system is deemed to be "slow" when its flushing time exceeds a tidal month, then Chesapeake Bay, Tomales Bay in summer, and the Satilla River are "slow" estuaries, while Tomales Bay in winter, the Columbia River, Waquoit Bay, and Plum is. Sound are "fast." Scalar transport processes in the Columbia River estuary vary both seasonally and over the tidal month. High riverflow and neap tides favor vertical mean shear dispersion, while low riverflow and spring tides favor vertical tidal shear dispersion. Tides are weaker in the Satilla River and other Georgia River systems than in the Columbia River. T_R is apparently governed by river flow and atmospheric processes.

Large variations in the T_R of Tomales Bay result from a seasonal alternation between a hypersaline state in summer and a positive estuarine circulation in winter. This seasonal change from lateral homogeneity to classical estuarine conditions is reflected in transport processes. Stratification is too small during the summer to sustain substantial vertical mean or tidal shear dispersion, and longitudinal exchange proceeds by lateral tidal shear mechanisms. The weakness of lateral shear-driven exchange processes may be a consequence of Tomales Bay's geological origin as a drowned fault. It is narrow (less than a tidal excursion wide at most locations) and lacks lateral embayments and projections.

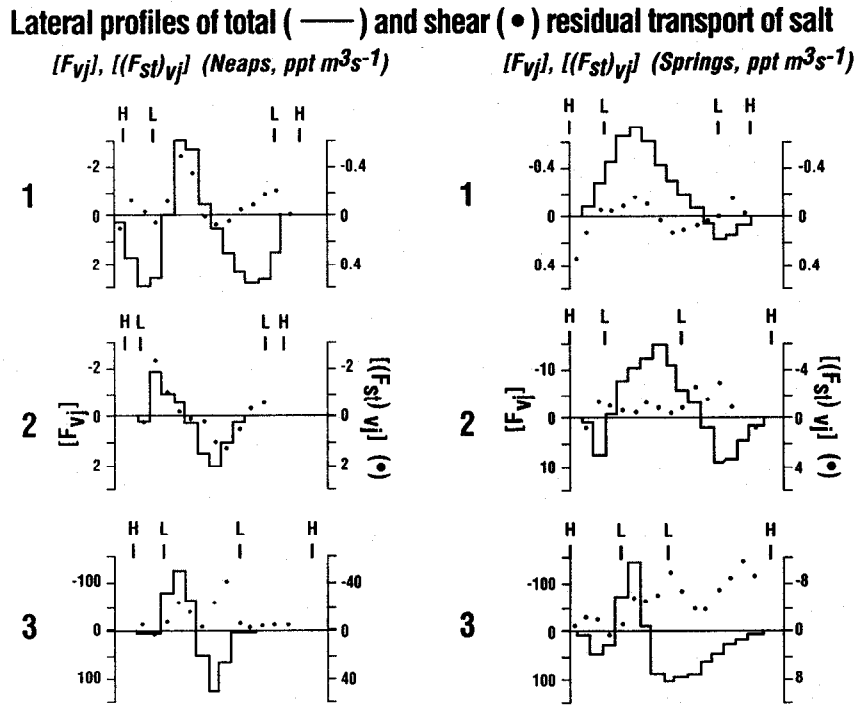


Fig. 4. Lateral variations in total net (—) and the transverse shear (•) contributions to salt transport in the Tamar Estuary.

Another important descriptor of estuarine transport processes is the continuous or intermittent nature of exchange with the coastal ocean. The Columbia River estuary is an example of a system that has a short flushing time, because it is strongly and continuously flushed by tidal action and freshwater inflow. Even though the salt balance is typically unsteady, atmospheric and episodic oceanic forcing (e.g., upwelling) are almost insignificant to

flushing because they cannot greatly reduce the very short flushing time.

Alternatively, mean horizontal fluxes may be small relative to scalar inventory, and flushing of a system can be largely caused by infrequent events. None of the LMER systems exhibit intermittent flushing to such a degree as silled fjords, but atmospheric forcing is of some importance in flushing all of the systems except the Columbia River.

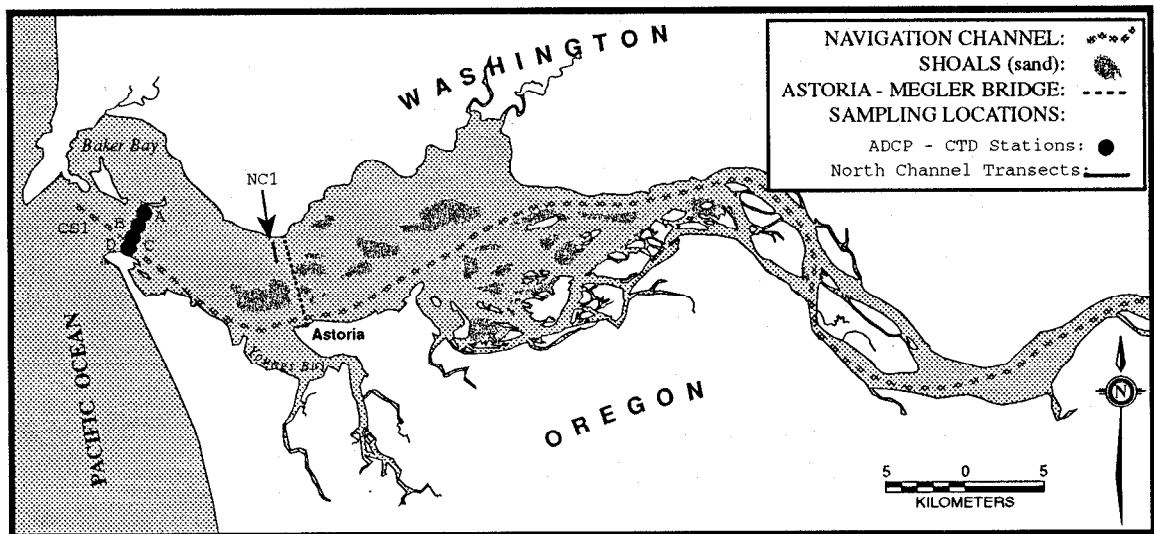


Fig. 5. Station location map for the Columbia River estuary, showing sections NC1 and CS1.

When a large system exhibits intermittent flushing, this usually means that its salt balance is nearly steady and T_R very long most of the time. Infrequent flushing events greatly reduce T_R and cause large, temporary imbalances in salt transport. Hurricanes in Chesapeake Bay are an extreme example of this phenomenon.

The "fast" or "slow" character of flushing plays an important role in definition of circumstances under which the direct and indirect flux calculations are applicable. The scalar flux calculation approach suggested in Table 2 is directly related to the T_R and character of flushing in each system. Our argument can be understood in terms of Eq. (1) and Eq. (2). Direct measurements cannot be used to determine scalar fluxes on the r.h. side of Eq. (1) or Eq. (2) in a large system with weak flushing (e.g., Chesapeake Bay) because logistics limit direct flux measurements to a maximum duration of a few days. Even if a flux significantly different from zero could be obtained, it would provide very little information concerning the behavior of scalars over a flushing time. Direct measurements are also unlikely to capture a rare, rapid flushing event that may have a large impact on such a system. The primary purpose of a direct flux estimation in these systems is to investigate the details of circulation and transport processes; atmospheric forcing on scales of ~ 3 – 10 d causes them, however, to exhibit discouragingly large variability (e.g., Weissburg 1976; Elliot and Wang 1978), requiring numerous flux determinations before a thorough understanding can be obtained. Indirect flux estimation is feasible in these systems precisely because their flushing time is large. The l.h. side of Eq. (1), averaged over a T_R , can either be taken as zero or measured (e.g., during a major flushing event). The fluxes on the r.h. side of Eq. (1) may then be determined by measurement of the non-conservative terms [the remainder of the r.h. side of Eq. (2)] or, in some cases, from the freshwater input or evaporative loss of fresh water for negative estuaries (Largier et al. In press).

At the other extreme, direct and indirect estimation of fluxes are both very difficult in a large stratified system with strong tides (e.g., the Columbia River estuary). Salinity and velocity gradients are sharp, and the estuarine inventory on the l.h. side of Eq. (1) exhibits strong tidal variability. Remote sensing of surface salinity is useless in determining the estuarine salt inventory because of strong and variable stratification. Whether a direct or indirect approach is employed, either an extensive moored-instrument array or several vessels would be required. Recent development of computer-controlled CTD packages that can be rapidly "tow-yowed" in shallow water may decrease these

difficulties. Measurement of fluxes in such systems is still, however, an expensive sampling exercise because of the amount of equipment and number of personnel required. Only indirect flux estimates are possible in most of Chesapeake Bay. But both direct and indirect flux estimation are probably feasible in Waquoit Bay, Plum Island Sound, and Tomales Bay in winter, the best method depending on the scalar of interest.

SCALAR TRANSPORT AND ESTUARINE CLASSIFICATION

It would also be desirable to develop a nondimensionalization scheme that allowed direct comparison of transports (and not just flux mechanisms) between estuaries. This question arises because it is not obvious how to compare fluxes in small estuaries like Waquoit Bay or Plum Island Sound, with surface areas of less than 10 km^2 , to those in much larger systems like Chesapeake Bay (area $11,500 \text{ km}^2$). One possibility would be to nondimensionalize T_R for scalars of ecological interest using either salt or fresh water T_R as a standard. The ratio, for example, of the T_R of silt in an estuarine turbidity maximum (ETM) normalized by that of water in the same estuarine volume would be an indicator of the particle trapping efficiency of the ETM.

Another unresolved issue is an extension of the first: the relationship of fluxes or transport mechanisms to estuarine classification schemes. The Hansen and Rattray (1966) system is a good example of how a useful connection might be made. Once an estuary is classified with this two-parameter system, a prediction of the balance between tidal and mean flow salt transport is readily derived. Unfortunately, unsteadiness of the salt balance and other factors render predictions of this model (and all available two-dimensional x-z models of estuarine circulation) suspect. Thus, despite its great breadth of vision, the Hansen and Rattray classification scheme confers only limited predictive capability for salt transport, and further theoretical work is needed. Finally, a salt balance model cannot be used to directly predict transport for scalars other than salt, because these scalars will be transported differently than salt unless their spatial distribution is exactly the same as that of salt (Jay 1995). This again suggests that additional estuarine classification parameters may be needed to describe processes such as particle trapping.

Flux Estimation Technologies and Approaches

FLUX ESTIMATES FROM ADCP/CTD DATA

An unprecedented resolution of the tidal, residual, and overtide components of the velocity field has been achieved through harmonic analyses of time series of moving-boat, narrow-band (NB-)

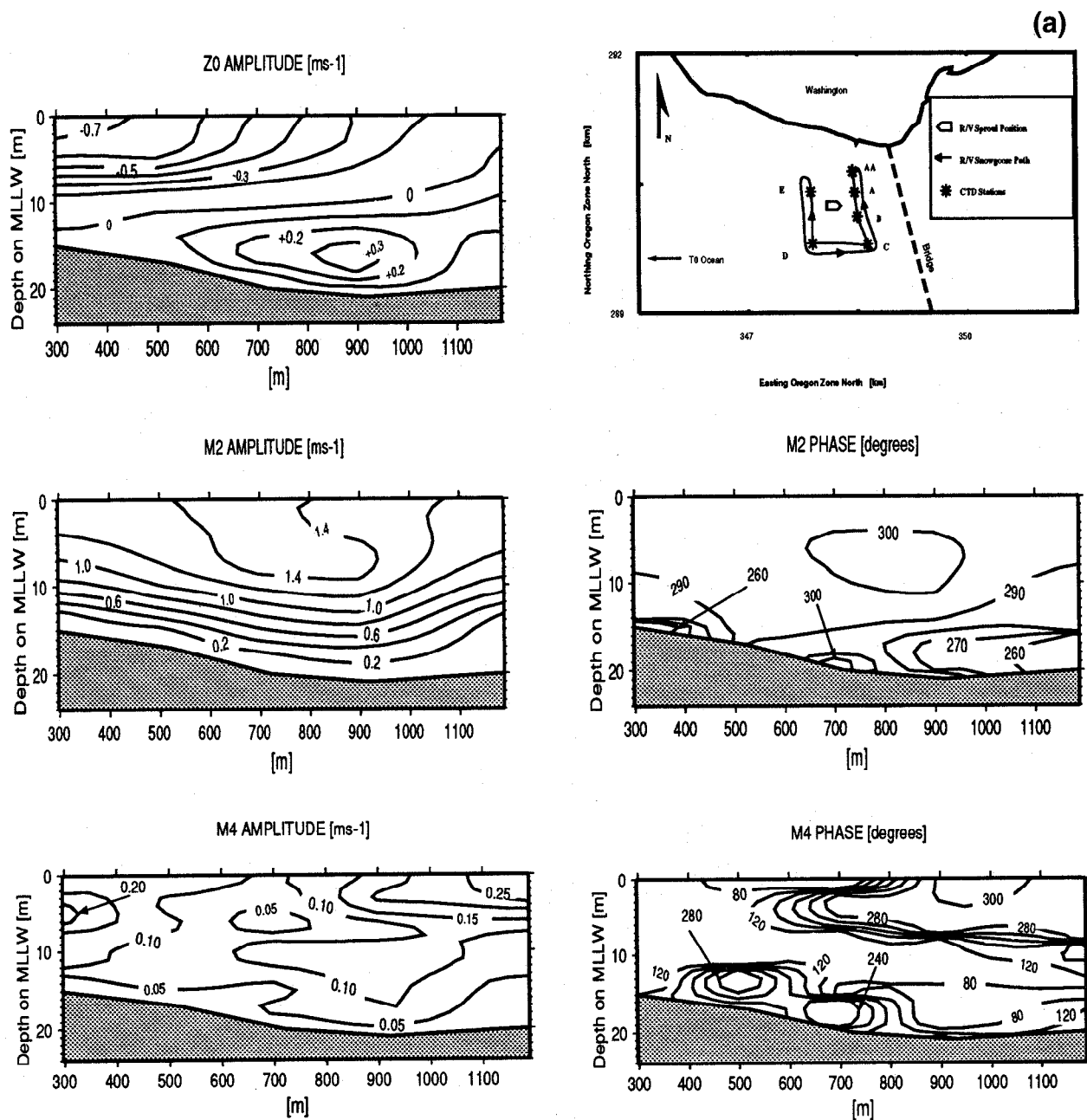


Fig. 6. (a) Cross-sectional distributions (looking landward) of along-channel mean (Z_0), M_2 and M_4 tidal current. (b) SPM at cross-section NCI in the turbidity maximum of the Columbia River estuary. Also shown in (a) is a sketch of the vessel sampling pattern used on section NCI [rightmost of two sections with four CTD stations shown by (*)], and another section with two CTD stations. Insufficient optical backscatter data were available for harmonic analysis at station AA on section NCI.

ADCP data (Geyer and Signell 1990; Geyer 1993; Jay and Musiak 1996). Nevertheless, the resolution of NB-ADCPs used to date falls short of what is needed to make meaningful scalar transport calculations in most systems. Their vertical resolution is limited by vertical sampling bin size (≥ 1 m), a partial overlap between bins in signal reception, and the instrument's inability to track the large

shear often found in estuarine environments. Horizontal resolution is limited to ~ 100 – 500 m by instrument sampling rate, a need to average numerous samples to reduce errors, and the speed of the sampling vessel necessary to achieve synoptic coverage. This resolution is too coarse to reveal lateral variability in the along-channel flow that in part governs scalar transport (Kjerfve and Proehl 1979,

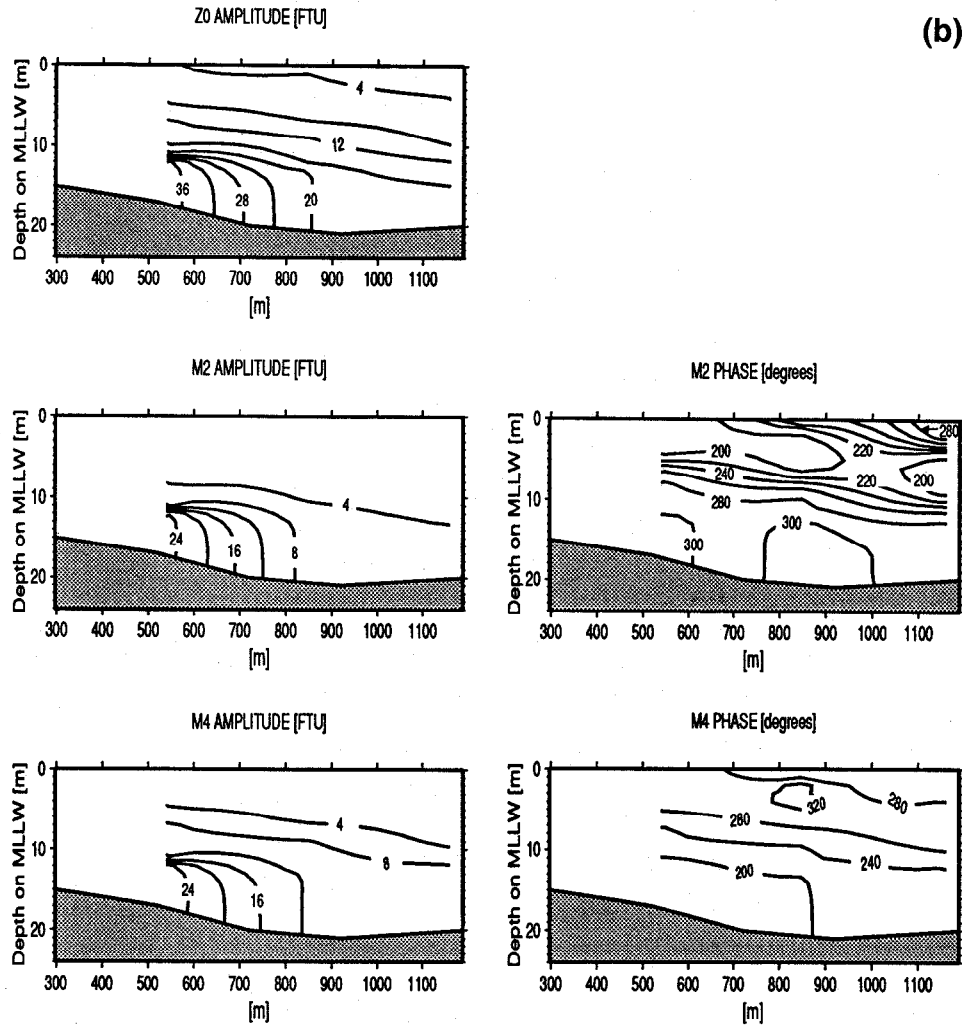


Fig. 6. Continued.

Uncles et al. 1985). A certain amount of the water column is also inaccessible to ADCP sampling: ~ 1 m plus the depth of the NB-ADCP transducers at the free surface and 15% of the depth at the bed (for a typical shipboard configuration with 30° beam angles). This is undesirable for salt transport analyses and unacceptable for sediment transport calculations.

Transport calculations based on data collected using a boat-mounted 1.2 mHz NB-ADCP and a CTD profiler nonetheless provide useful information concerning scalar transport calculation methods, as illustrated by a study in the Columbia River estuary (Kay et al. In press). Transport calculations were made for transect CS-1 near the mouth of the Columbia River using data collected July 27–28, 1992 (Fig. 5). (Near-bed flux estimates are based on velocity profiles extrapolated to the bed using a momentum balance model with an eddy-diffusivity turbulence closure with stratification correc-

tion.) River flow was $\sim 60\%$ of annual average, and tidal forcing was weak. For purposes of averaging the velocity, the section was divided into four “boxes” of ~ 250 m width, with a CTD station centered in each. The resultant salinity and velocity records were subjected to harmonic analysis, and the transport determined as a sum of transports associated with the mean flow and the first eight tidal species.

Calculations suggest that division of the section into four boxes was sufficient to achieve a water balance accurate to $\pm 7\%$. The salt balance caused greater difficulty. A net inward salt flux of $\sim 60\%$ of the outward transport by the mean flow $A\langle\{U\}\rangle\langle\{C\}\rangle$ was calculated at CS-1 using a balance similar to Eq. (8). Employment of a GLM assumption caused a marked change in the result; Eq. (9) yielded a net outward transport of $\sim 36\%$ of $A\langle\{U\}\rangle\langle\{C\}\rangle$. Comparison of mean salinities before and after the calculation period suggest there was a small (relative to either of these results) net

TABLE 2. Estuarine flux characteristics of selected LMER systems.

	Chesapeake Bay	Tomales Bay	Waquoit Bay	Columbia River	Satilla River	Plum Island Sound
Dominant flux mechanism	VMSD ^a	VMSD + LTSD (wi. ^f) LTSD ^b (su.)	VMSD (tributaries) Variable (bay)	VTSD ^{c,e} (low flow) VMSD + VTSD (high flow)	?	VMSD (Parker River) LTSD (Sound)
Residence time	3–9 mo	1–100 d (su. ^f) 0.5–5 d (wi.)	0.5–4 d	3–5 d (low flow) 1–3 d (high flow) ^d	120 d (mean flow) 71 d (high flow)	? (Parker River) 0.5 d (Sound)
Character of flushing	Continuous + intermittent	Continuous; intermittent in wi.	Continuous + intermittent	Continuous	Continuous + intermittent	Intermittent (Parker R., su.) Continuous (Parker R., wi.) Continuous (Sound)
Suggested flux calculation approach	Indirect	Indirect (su.) Both (wi.)	Both	Direct	Both	Both

^a VMSD = vertical mean flow shear dispersion.

^b LTSD = lateral tidal shear dispersion.

^c VTSD = vertical tidal shear dispersion.

^d Neal (1972).

^e Hansen (1965), Jay and Smith (1990).

^fwi. = winter, su. = summer.

landward salt transport, and both imbalances are too large to be explained by the net water transport. Use of the GLM assumption was not clearly beneficial. But in contrast, if one applies the GLM approach Eq. (9) to the data of Hughes and Rattray (1980) for this section, then there is a considerable improvement in the result (i.e., a net salt balance much closer to zero is achieved). In our case, measurements were made during periods of large and rapid fluctuations in riverflow associated with upstream reservoir manipulation. The contribution of a nonstationary salt balance to the discrepancy between inward and outward salt transport and the difference in results between Eq. (8)

and Eq. (9) is unclear, but a systematic sampling error (discussed below) was also likely present.

Flux calculation results are only useful if they can be interpreted, and some aspects of these results are consistent with prior work. Figure 7 shows that tidal salt transport ($\sum_j \overline{U_j C_j}$) is landward throughout the section and is greatest above mid-depth, in a part of the flow where tidal salinity variations are large. It is particularly strong at stations A and B, where tidal currents are strongest. Mean flow salt transport (\overline{UC}) is maximal and most seaward along the south side of the estuary, at station D in the navigation channel. These findings are consistent with the transports at this section calculated by Jay and Smith (1990) from moored current meter data, and with results of Hughes and Rattray (1980). All analyses taken together suggest that this distribution of salt fluxes is persistent, regardless of fluctuations in riverflow and tidal range. It is in part a result of engineering efforts to concentrate riverflow in the navigation channel, minimizing dredging. It also reflects a basic topographic reality—channel curvature near the mouth of the estuary amplifies and rectifies tidal currents along the north side of the system. Thus, most of the tidal prism (including that over large mid-estuary sand flats) fills from the north channel, and this naturally causes strong salinity intrusion in that channel.

The character of the shear fluxes is also consistent with theoretical expectations (Jay 1991). Mean and tidal vertical shear fluxes were landward at all depths and frequencies (Fig. 8), though there was substantial cross-channel variability in the ab-

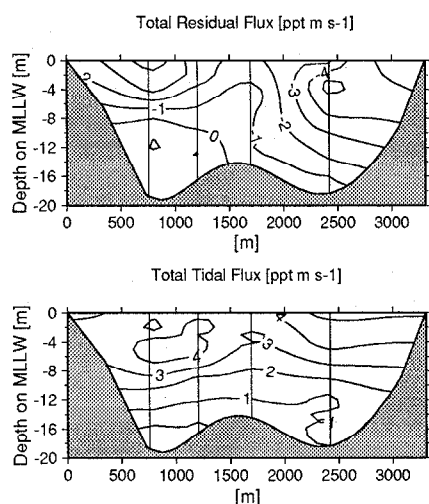


Fig. 7. Spatial distribution of mean and tidal salt fluxes \overline{UC} and $\sum_j \overline{U_j C_j}$ on section CS1, looking landward.

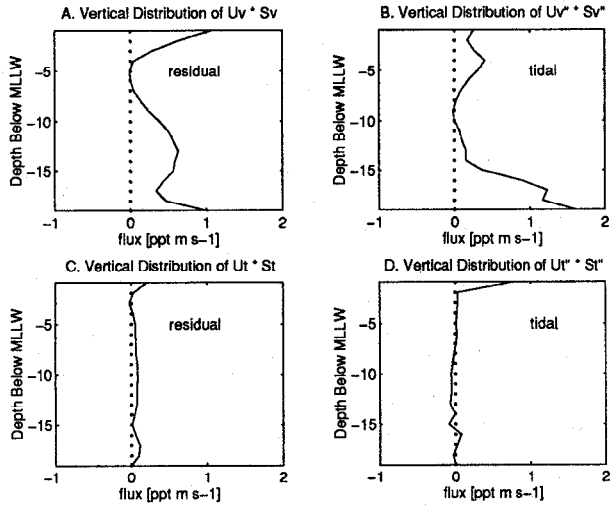


Fig. 8. The vertical distribution (top panel) of mean and tidal contributions to the vertical shear salt transport $\langle \bar{U}_v \rangle \langle \bar{C}_v \rangle$ and $\sum_j \langle \bar{U}_{vj} \rangle \langle \bar{C}_{vj} \rangle$ on section CS1 near the mouth of the Columbia River estuary. The same is shown in the lower panel but for lateral shear transport $\langle \bar{U}_b \rangle \langle \bar{C}_b \rangle$ and $\sum_j \langle \bar{U}_{bj} \rangle \langle \bar{C}_{bj} \rangle$.

solute size of the salt transports. There was also a spectral structure to the salt transport that comes directly from the character of the velocity field. M_2 currents are typically two to five times larger than those at K_1 , and the mean (Z_0) shear is also larger than K_1 currents. Not surprisingly, Z_0 and M_2 vertical shear-flux terms $\langle \bar{U}_v \rangle \langle \bar{C}_v \rangle$ and $\langle \bar{U}_{2v} \rangle \langle \bar{C}_{2v} \rangle$ dominated the vertical shear fluxes, $\langle \bar{U}_{vb} \rangle \langle \bar{C}_{vb} \rangle$; ea and $\langle \bar{U}_{2vb} \rangle \langle \bar{C}_{2vb} \rangle$ were the largest of the vertical-lateral shear fluxes, and $\langle \bar{U}_b \rangle \langle \bar{C}_b \rangle$ and $\langle \bar{U}_{b2} \rangle \langle \bar{C}_{b2} \rangle$ (though small) were larger than the other integral lateral shear fluxes. K_1 and M_4 shear fluxes were a little larger than those at the remaining frequencies. The minor importance of diurnal fluxes (relative to Z_0 and M_2) is fortunate, because experiments with artificial data show that semidiurnal and higher frequency constituents are much easier to correctly determine from a short record via harmonic analysis than K_1 (Jay and Flinchem 1997).

If Eq. (9) is correct, then the total transports shown in Fig. 7 are somewhat deceptive, because they contain within them large terms of opposite sign. Indeed, the shear flux distributions in Fig. 8 are very different from the total fluxes in Fig. 7. Figure 8 shows the vertical distribution of mean and tidal contributions (sum of all constituents) to the vertical and lateral shear-flux terms, averaged across the entire flow width. Mean (Z_0) vertical shear fluxes are landward at all depths but most sharply so very close to the bed and free surface. The near-bed flux represents landward movement of high-salinity water, while the near-surface flux results from seaward transport of low-salinity water. The tidal vertical shear flux is greatest very close

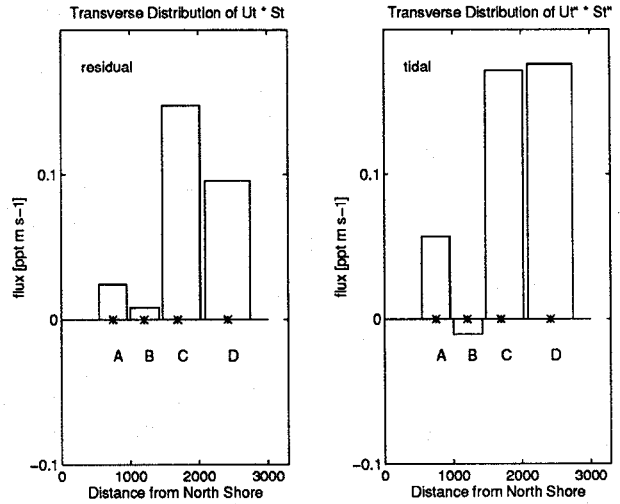


Fig. 9. Lateral variation in contributions to mean and tidal lateral shear salt transports $\langle \bar{U}_b \rangle \langle \bar{C}_b \rangle$ and $\sum_j \langle \bar{U}_{bj} \rangle \langle \bar{C}_{bj} \rangle$ on section CS1 near the mouth of the Columbia River estuary for stations A, B, C, and D (from north to south across the section).

to the bed and comes almost totally from M_2 ; other species are insignificant. The lateral shear contributions in Fig. 8 are, averaged across the channel, small except very close to the bed and free surface. Figure 9 shows that the vertically integrated contributions to mean and tidal lateral shear salt transport are much smaller than one might guess from Fig. 7. This appearance may be incorrect, however, because of a sampling problem discussed below.

There are several lessons to be learned from these results: First, a large error in flux calculations can be caused by seemingly minor logistical decisions. In our case the calculated net landward transport [via Eq. (8)] appears to have been larger than justified by temporal changes in salt inventory, and the sampling scheme provide a likely explanation. The observations failed to include most of parts of transects that were less than 9 m deep. The flow in these areas probably contributes to landward salt transport because of a strong net seaward movement of low-salinity water, particularly along the beach at the south end of section CS-1. This measurement bias is not easily avoided in a large estuary with broad tidal flats—the speed and vessel stability necessary for sampling deeper channels makes sampling of shallow subtidal and intertidal areas very difficult. If sampling transects cannot be chosen to avoid this problem, a second vessel should be used to sample in shallow water. Second, the sensitivity of the net transport to substantial errors from seemingly small sampling biases results arises from its quadratic nature. That is, if biases imposed on the individual variables (velocity and salt) are correlated, errors in transport may be considerably larger than errors in the

mean salinities and velocities taken individually. In our case, shallow water areas were fresher and had stronger outflow. Incorporation into a transport expression analogous to Eq. (4) or Eq. (5) of tidal variations in width under a "small-amplitude" assumption (analogous to that used for variations in surface elevation) might provide at least a means of estimating the errors involved in neglecting flows over tidal flats. Third, CTD profile data from isolated stations are likely to be inadequate for transport calculations. On transect CS-1, for example, sufficient ADCP data were available to divide along-channel velocities into nine boxes across the channel, but only four CTD stations were occupied, limiting the utility of the ADCP data. Either the CTD must be "tow-yowed," or a vessel must be devoted exclusively to CTD sampling. Dense sampling is necessary to achieve both statistically significant net transports and to allow error estimation via subsampling. Fourth, strong near-bed and near-surface excursions of the shear-stratification correlations for the mean flows points out the importance of accurate sampling near the bed and free surface. Fifth, Most estuarine current and scalar time series are statistically nonstationary, due to the influences of fluctuating winds, river inflow, and oceanic density conditions. When the influence of nonstationary processes with periods of less than ≈ 10 d is reflected in current and/or scalar records harmonic analysis of short (25–100 h) time series can lead to serious errors in current and/or scalar amplitudes and phases (Jay and Flinchem 1997). Extraction of tidal species information using continuous wavelet transforms is more accurate than harmonic analysis for any given record length. However, longer records than used in most previous transport studies (≥ 100 h for the diurnal and 50 h for the semidiurnal tide) are required for accurate determination of tidal quantities whatever analysis method is employed, and there is a need to develop methods for estimating errors in such analyses.

IMPROVEMENTS IN TECHNOLOGY

There are now at least five firms in the ADCP market. This has spurred improvements in technology and price decreases. Recent development of broad-band (BB-)ADCP and higher-frequency NB-ADCPs for vessel use suggests the possibility of achieving a fuller three-dimensional knowledge of the estuarine velocity field down to the scale of large eddies and internal instabilities. Increasing the frequency of an NB-ADCP improves resolution and precision through use of shorter waves but at the cost of a smaller depth range. A BB-ADCP accomplishes the same ends by sending out a more complex signal. For either NB or BB instruments,

smaller vertical bin sizes, larger transducers (or synthetic transducer arrays), and smaller beam angles allow data acquisition closer to the bed and free surface, and better precision improves horizontal resolution by decreasing averaging time. Thus, horizontal resolution should in most cases be limited to a small multiple of the distance between opposite pairs of slant beam (72% of sample depth for a 20°-beam angle configuration) rather than by horizontal vessel motion over a lengthy averaging period.

A lack of very near surface data could be eliminated through use of a CTD and a current meter mounted on a small boat, or by an ocean-surface radar system (Matthews et al. 1990) coupled with airborne electromagnetic (AEM) measurements of the conductivity (and thus density) field. AEM, employed for >40 yr in geophysical prospecting, has recently been used to determine bathymetry, sea-ice thickness, and vertically averaged conductivity (Won and Smits 1986; Kovacs and Valleau 1990). It can likely also be used to calculate simple vertical conductivity distributions, but this has yet to be demonstrated.

Thus, the most serious velocity sampling problem is the absence of data near the bed. This loss can be reduced from 15% of depth for 30° beam angles (usually employed older by boat-mounted NB-ADCPs) to ~ 5 –8% of depth for an ADCP with beams oriented more closely to the vertical. A reasonable scheme for extrapolation of velocity to the bed will probably render this loss of near-bed data unimportant for transport calculations involving scalars like salt, with their variability concentrated near mid-depth.

There are several qualifications to the above optimistic picture of ADCP velocity measurement capabilities. First, use of BB-ADCP and higher-frequency NB-ADCPs carries a stiff price in terms of data processing. The data collected by an older 1.2 MHz NB-ADCP are typically $O(5\text{--}15 \text{ Mb d}^{-1})$ in raw, binary form for a 10–20 m deep flow. New instrumentation operated at maximum sampling rate will increase this by a factor of 5 to 25. Achievement of maximum horizontal resolution will also require use of differential Global Positioning System (dGPS) navigation rather than normal GPS, usually implying extensive post-cruise data reduction.

Moreover, there is not yet available a comprehensive analysis of errors associated with the entire shallow-water sampling system; that is, ADCP, navigation system, tilt sensors, compass, and vessel. Reduction or elimination of the various errors associated with the ADCP itself will likely bring to the fore errors caused by other parts of the system; for example, the effect of vessel turns on the compass

used with the ADCP. Also, the utility of various vessel configurations needs to be re-evaluated. Optimal ADCP sampling puts a high premium on both vessel stability and shallow draft. Because of improvements in the bottom tracking software used by the ADCP, the optimum speed of vessel motion may either be greater than that available on some vessels or cause unsatisfactory boat wake effects. Finally, improved sampling of the velocity field requires a comparable improvement in the density of scalar observations, if realistic transport results are to be obtained.

The possible ability of ADCPs to measure SPM concentration has also been little exploited. An ADCP determines velocity from measurement of Doppler shift. Acoustic backscatter intensity information acquired in the process is normally treated as an incidental variable and neglected; this is unfortunate. The potential value of ADCP backscatter intensity as a means to measure SPM lies in the exact correspondence of the scale and sampling interval of the resultant velocity and SPM estimates. Jay and Musiak (1996) and Thevenot and Kraus (1993) have shown the feasibility of calibrating ADCP backscatter (rather than the backscatter of individual beam measurements) against optical backscatter (OBS) estimates of SPM as an intermediate calibration step. A final calibration against direct SPM measurements is, of course, essential.

The practical utility of ADCPs to calculate SPM transport remains to be demonstrated. Except for washload fractions that do not play an active role in estuarine ecodynamics, SPM transport is usually concentrated in the part of the water column for which no ADCP data are available. Moreover, there is also no guarantee that the above relationship between SPM and backscatter will be sufficiently linear or constant in time to be useful, and NB-ADCP backscatter saturates at a relatively low concentration ($\sim 60\text{--}100\text{ mg l}^{-1}$ in the Columbia River). Other instruments, for example, tripod-mounted current meters and optical backscatter systems, may provide the missing, near-bed velocity and SPM data at isolated times and/or locations but not with the time and space resolution needed for sediment transport calculations. SPM is, therefore, a prime example of a scalar for which flux calculations may require a joint observational and numerical modeling approach.

FLUX CALCULATION METHODOLOGY

Another possible approach to improving the calculation of cross-sectional scalar fluxes is to use GLM ideas concerning Lagrangian transport to simplify expansions [as in derivation of Eq. (9) from Eq. (2)] of net scalar transport and to improve inclusion of lateral variations, including

those in channel width. The GLM approach has several potential advantages; it clearly identifies the terms responsible for landward transport of scalars; minimizes the number of terms in the transport expansion, allowing inclusion of as many tidal constituents as can be resolved in the velocity and scalar data; can readily be extended to scalars that settle or are nonconservative; and allows use of the same balance in data analyses, box models, and theoretical calculations.

Aside from the calculations discussed above, this approach has only been used to analyze T_R calculation methods (Jay 1995) and the mechanisms causing particle trapping in tidal channels (Jay and Musiak 1994). Its practicality for computing transports from field data and the fundamental correctness of the underlying theory (i.e., the relationship for weakly nonlinear waves between Stokes drift transport of a mean scalar field and wave transport of tidal scalar variability) has only recently undergone preliminary testing. The initial results discussed above and by Kay et al. (1996) are inconclusive, and further tests on a more detailed dataset is required. Further work is needed, moreover, in defining a theoretical basis for analyzing transport in truly three-dimensional water bodies, where there is no axis of freshwater discharge and the fraction of the flux that contributes to changing the scalar distribution may only be a small fraction of the total flux (Middleton and Loder 1989). Finally, better statistical analyses of transport calculations are vital.

NUMERICAL MODELS AND FLUX CALCULATION

Numerical models also offer hope for improvement of cross-sectional scalar transport, because errors related to under-sampling can be avoided in flux calculations based on model results. Baird et al. (1987), for example, used a one-dimensional, cross-sectionally averaged flow model and observations to calculate export of SPM from the Swartkops Estuary, South Africa. The most complex example to date of use of numerical models to determine estuarine transport appears to be calculations for the Hudson River estuary carried out by Oey et al. (1985). This study was entirely numerical and employed three-dimensional circulation and scalar transport models. Still, there is considerable latitude for development of more sophisticated methods for combining flow models and observations of scalar transport.

Important questions also remain to be answered concerning the ability of numerical models to predict the consequences of anthropogenic changes in estuarine processing and transport of ecologically relevant scalars. Such predictions will likely require models that have been tested and verified

to an unusually high standard. These models must not only conserve scalars over long time periods. They must, if they are to have predictive capabilities, reproduce scalar concentration fluctuations and each individual transport mode correctly. Unfortunately, scalar transport is a nonlinear, second-order quantity that is inherently sensitive to small errors in either the velocity or salinity field. An obvious example is the tidal-cycle average of tidal transport of a scalar, which may be represented as $|U| |C| \cos \Delta$, where $|U|$ is tidal velocity amplitude, $|C|$ tidal scalar amplitude, and Δ the phase difference between tidal salinity and velocity variations. For many scalars like salinity, Δ is close to 90° and even a small error in Δ may result in a completely erroneous estimate of scalar transport. Thus, it may be more difficult to calibrate a model to determine scalar transport with an acceptable degree of accuracy than it is for velocity and scalar concentration individually. Moreover, extraction of accurate tidal species phases and amplitudes from numerical model runs is, just as with field data, a problem for both velocity and scalar concentration. This is true even though under-sampling can be avoided in modeling—the largest harmonic analysis errors in phase and amplitude for quantities whose true amplitude is non-zero are related to nonstationary behavior of the scalar and velocity fields, not under-sampling.

Recommendations and Conclusions

The need to measure, understand, and predict particle and solute fluxes to and from estuaries and bays has led to a wide diversity of studies and methodologies. In this article, we have discussed the problems associated with estimates of scalar fluxes. Of particular concern are the common circumstances where one wishes to a) measure a net flux that is small relative to flood and ebb transports; or b) determine the effect of source and sink terms that are small relative to the tidal influx and efflux (often the case with anthropogenic inputs). In either situation, errors in the estimate may swamp the desired result. Development of rigorous estimates of a net estuarine scalar flux require improved monitoring of inputs, an improved conceptual framework, comparison of measurements with basin-scale monitoring and numerical modeling, and diagnostic “smart” observation strategies for scalar concentrations, perhaps derived through numerical experiments.

Inputs of water, SPM, nutrients, and other substances are seldom well known. The United States Geological Survey maintains an extensive network of hydrological stations to monitor rivers, but there is an absence of coordinated programs to monitor inputs to estuaries and bays, particularly from

groundwater. Input terms should be monitored at the boundary of the system, and Eq. (9) reminds us of the importance of knowing riverflow in calculating fluxes.

Many estuaries exhibit substantial scalar input variability at time scales from a few hours to days, and these changes are often sufficiently large that a scalar balance (e.g., for salt or sediment) may be quite unsteady. Lateral scalar concentration and flux variabilities and their relationship to topography, stratification, and circulation are also not well understood. Furthermore, the relative importance of different transport mechanisms in various types of estuaries has yet to be well described, and an improved conceptual framework is required in the study of scalar transport in wide shallow estuaries that have time-varying surface area and/or do not have an obvious axis of river discharge and tidal propagation.

Finally, we suggest that an interdisciplinary flux experiment be conducted to evaluate recent improvements in instrumentation and flux calculation methods. For the sake of argument, we recommend carrying out this project in Tomales Bay during spring, before hypersaline conditions are established. The topography of Tomales Bay is perhaps simpler than that of any comparably sized system in the United States. Most important, however, is the ability to apply both direct and indirect methods—simultaneous determination of cross-sectional fluxes and basin scalar inventories would allow a comparison of these two methods, something that has never before been carried out in a systematic manner. Such an experiment should cover a significant fraction of the T_R for salt during both spring and neap tides. In addition to measurements related to water, salt, and heat transports, measurements might include dissolved oxygen, chlorophyll (by fluorometer), nutrient, plankton, and SPM concentrations.

The sampling routine would also need to address the mismatch between the time and space scales of biogeochemical measurements and those of physical measurements. It is unrealistic to expect to measure biogeochemical fields at the same rate at which ADCP or CTD sensors measure physical fields, and one must determine “smart” approaches to measuring the biogeochemical fields. This might involve the use of physical measurements to interpolate the sparser biogeochemical data and/or the measurement of biogeochemical fields in a diagnostic, hypothesis-testing manner. Several vessels would be required for this experiment so that flux and basin-inventory measurements could proceed simultaneously for both physical and biogeochemical parameters. Salt inventory

changes might best be determined using airborne electromagnetic methods.

Following the experiment, the flow and transport results should be imported into a three-dimensional numerical model. Ideally, this model would be set up and calibrated prior to the experiment so that it could be used in the design of optimal sampling strategies. Such an experiment would not only help to determine the state-of-the-art of methodology for determining scalar fluxes to and from estuaries, it would also help develop the research community's conceptual framework for study of estuary-ocean biogeochemical fluxes.

ACKNOWLEDGMENTS

Preparation of this paper was supported by National Science Foundation LMER grants OCE-8918193 for the Columbia River Estuary, OCE-8914729 for Waquoit Bay, OCE-8914729 for Tomales Bay, OCE-9214461 for Plum Island Sound, and BED-8812113 for Chesapeake Bay. The first author was at the University of Washington, Geophysics Program, Seattle, Washington during preparation of the paper. Credit is due to J. D. Musiak and D. J. Kay for ADCP/CTD data processing and transport calculations; Mr. Musiak's analysis was supported by ONR grant N00014-94-1-0009. Thanks to C. Alexander and J. Blanton of Skidaway Institute for information concerning the Georgia rivers systems.

LITERATURE CITED

- ANDREWS, D. G. AND M. E. MCINTYRE. 1978. An exact theory of nonlinear waves on a Lagrangian-mean flow. *Journal of Fluid Mechanics* 89:609-646.
- BAIRD, D. P., E. D. WINTER, AND G. WENDT. 1987. The flux of particulate material through a well mixed estuary. *Continental Shelf Research* 7:1399-1403.
- BOON, J. D. 1978. Suspended solids transport in a salt marsh creek—An analysis of errors, p. 147-159. In B. Kjerfve (ed.), *Estuarine Transport Mechanisms*. Belle W. Baruch library in Marine Science, no. 7. University of South Carolina Press, Columbia, South Carolina.
- BOWDEN, K. F. 1963. The mixing processes in tidal estuary. *International Journal of Air and Water Pollution* 7:343-356.
- BOYNTON, W. R., W. M. KEMP, AND C. G. OSBORNE. 1980. Nutrient fluxes across the sediment water interface in the turbid zone in a coastal plain estuary, p. 93-109. In V. S. Kennedy (ed.), *Estuarine Comparisons*. Academic Press, New York.
- DRONKERS, J. J. AND J. VAN DE KREEKE. 1986. Experimental determination of salt intrusion mechanisms in the Volkerak Estuary. *The Netherlands Journal of Sea Research* 20:1-19.
- DUNKERTON, T. 1981. A Lagrangian mean theory of wave, mean-flow interaction with applications to non-acceleration and its breakdown. *Reviews of Geophysics and Space Science* 18:387-400.
- DYER, K. R. 1973. *Estuaries: A Physical Introduction*. J. Wiley and Sons, London, England.
- DYER, K. R. 1974. The salt balance in stratified estuaries. *Estuarine and Coastal Marine Science* 2:275-281.
- DYER, K. R., W. K. GONG, AND J. E. ONG. 1992. The cross sectional salt balance in a tropical estuary during a lunar tide and a discharge event. *Estuarine, Coastal and Shelf Science* 34:579-591.
- ELLIOT, A. J. AND D.-P. WANG. 1978. The effect of meteorological forcing on Chesapeake Bay: The coupling between an estuarine system and its adjacent coastal waters, p. 127-146. In J. C. J. Nihoul (ed.), *Hydrodynamics of Estuaries and Fjords*. Elsevier, Amsterdam.
- FISCHER, H. B. 1976. Mixing and dispersion in estuaries. *Annual Review of Fluid Mechanics* 8:1070133.
- GEYER, W. R. 1993. Three-dimensional tidal flow around headlands. *Journal of Geophysical Research* 98:955-966.
- GEYER, W. R. AND R. P. SIGNELL. 1990. Measurement of tidal flow around a headland with a shipboard acoustic Doppler current profiler. *Journal of Geophysical Research* 95:3189-3198.
- HANSEN, D. V. 1965. Salt balance and circulation in partially mixed estuaries, p. 45-51. In *Estuaries*, Publication No. 83, American Association for the Advancement of Science, Washington, D.C.
- HANSEN, D. V. AND M. RATTRAY, JR. 1965. Gravitational circulation in straits and estuaries. *Journal of Marine Research* 23:104-122.
- HANSEN, D. V. AND M. RATTRAY, JR. 1966. New dimensions in estuary classification. *Limnology and Oceanography* 11:319-326.
- HUGHES, F. W. AND M. RATTRAY, JR. 1980. Salt flux and mixing in the Columbia River estuary. *Estuarine and Coastal Marine Science* 10:479-493.
- JAY, D. A. 1991. Estuarine salt conservation: A Lagrangian approach. *Estuarine, Coastal and Shelf Science* 32:547-565.
- JAY, D. A. 1995. Residence time, box models and shear fluxes in tidal channel flows, p. 3-12. In K. R. Dyer, and R. J. Orth (eds.), *Changes in Fluxes in Estuaries*. Olsen and Olsen, Fredensborg.
- JAY, D. A. AND E. P. FLINCHEM. 1997. Interaction of fluctuating river flow with a barotropic tide: A demonstration of wavelet tidal analysis methods. *Journal of Geophysical Research*. 102:5705-5720.
- JAY, D. A. AND J. D. MUSIAK. 1996. Internal tidal asymmetry in channel flows: Origins and consequences, p. 219-258. In C. Pattiaratchi (ed.), *Mixing Processes in Estuaries and Coastal Seas*. American Geophysical Union, Coastal and Estuarine Sciences Monograph, Washington, D.C.
- JAY, D. A. AND J. D. MUSIAK. 1994. Particle trapping in estuarine turbidity maxima. *Journal of Geophysical Research* 99:20,446-20,461.
- JAY, D. A. AND J. D. SMITH. 1990. Circulation, density distribution and neap-spring transitions in the Columbia River Estuary. *Progress in Oceanography* 25:81-112.
- KAY, D. J., D. A. JAY, AND J. D. MUSIAK. 1996. Salt transport through an estuarine cross-section calculated from moving vessel ADCP and CYD data, p. 195-212. In D. G. Aubrey and C. T. Fredericks (eds.), *Bouyancy Effects in Estuaries*. American Geophysical Union, Coastal and Estuarine Sciences Monograph, Washington, D.C.
- KALKWIK, J. P. T. AND R. BOOIJ. 1986. Adaptation of a secondary flow in nearly horizontal flow. *Journal of Hydraulic Engineering* 24:19-37.
- KJERFVE, B. AND J. A. PROEHL. 1979. Velocity variability in a cross-section of a well-mixed estuary. *Journal of Marine Research* 37:409-418.
- KOVACS, A. AND N. C. VALLEAU. 1990. Airborne electromagnetic measurement of sea-ice thickness and sub-ice bathymetry, In D. V. Fitterman (ed.), *Development and Applications of Modern Airborne Electromagnetic Survey Techniques*. *United States Geological Survey Bulletin* 1925:165-169.
- LARGIER, J. L., J. T. HOLLIBAUGH, S. V. SMITH, AND C. J. HEARN. In press. Seasonally hypersaline estuaries—finely balanced ecosystems. *Estuarine, Coastal and Shelf Science*.
- LEWIS, R. E. AND J. O. LEWIS. 1983. The principal factors contributing to the salt flux in a narrow, partially stratified estuary. *Estuarine and Coastal Marine Science* 16:599-626.
- MURRAY, S. P. AND A. SIRIPONG. 1978. Role of lateral gradients and longitudinal dispersion in the salt balance of a shallow, well-mixed estuary, p. 113-124. In B. Kjerfve (ed.), *Estuarine Transport Mechanisms*. Belle W. Baruch library in Marine Science, no. 7. University of South Carolina Press, Columbia, South Carolina.

- LMER COORDINATING COMMITTEE. 1992. Understanding changes in coastal environments: The LMER program. *EOS* 73:481, 484-485.
- MATTHEWS, J. P., D. PRANDLE, AND J. H. SIMPSON. 1990. Measurement of residual currents in the coastal zone with OSCAR HF radar: A review of results from the May 1985 experiment, p. 413-430. In R. T. Cheng, (ed.), *Residual Currents and Long-term Transport*. Springer-Verlag, New York.
- MIDDLETON, J. F. AND J. W. LODER. 1989. Skew fluxes in polarized wave fields. *Journal of Physical Oceanography* 19:68-76.
- NEAL, V. T. 1972. Physical aspects of the Columbia River and its estuary, p. 19-40. In A. T. Pruter and D. L. Alverson (eds.), *The Columbia River Estuary and Adjacent Coastal Waters*. University of Washington Press, Seattle, Washington.
- OFFICER, C. B. 1976. *Physical Oceanography of Estuaries (and Associated Coastal Waters)*. John Wiley and Sons, New York.
- OYEY, L.-Y., G. L. MELLOR, AND R. I. HIRES. 1985. A three-dimensional simulation of the Hudson-Raritan Estuary. Part III: Salt flux analysis. *Journal of Physical Oceanography* 15:1711-1720.
- RATTRAY, M., JR. AND R. J. UNCLES. 1983. On the predictability of the ^{137}Cs distribution in the Severn Estuary. *Estuarine, Coastal and Shelf Science* 16:475-487.
- REED, D. AND J. DONOVAN. 1994. The character and composition of the Columbia River estuarine turbidity maximum, p. 445-450. In K. R. Dyer, (ed.), *Changing Particle Fluxes in Estuaries: Implications from Science to Management*. Olsen and Olsen, London.
- SMITH, J. D. 1977. Modeling sediment transport on continental shelves, p. 539-572. In E. D. Goldberg, I. N. McCave, J. J. O'Brien, and J. H. Steele, (eds.), *The Sea: Ideas and Observations*, Vol. II. Wiley Inter-Science, New York.
- SMITH, S. V., J. T. HOLLIBAUGH, S. J. DOLLAR, AND S. VINK. 1991. Tomales Bay metabolism: C-N-P stoichiometry and ecosystem heterotrophy at the land-sea interface. *Estuarine, Coastal and Shelf Science* 33:223-257.
- THEVENOT, N. M. AND N. E. KRAUS. 1993. Comparison of acoustic and optical measurements of suspended particulate matter in Chesapeake Bay estuaries. *Journal of Marine Environmental Engineering* 1:65-79.
- UNCLES, R. J., R. C. A. ELLIOTT, AND S. A. WESTON. 1985. Dispersion of salt and suspended sediment in a partly mixed estuary. *Estuaries* 8:256-269.
- WEISSBERG, R. H. 1976. The nontidal flow in the Providence River of Narragansett Bay: A partially mixed estuary. *Journal of Physical Oceanography* 6:345-354.
- WEST, J. R., R. J. UNCLES, J. A. STEPHENS, AND K. SHIONO. 1990. Longitudinal dispersion processes in the Upper Tamar Estuary. *Estuaries* 13:118-124.
- WINTERWERP, J. C. 1983. Decomposition of the mass transport in narrow estuaries. *Estuarine, Coastal and Shelf Science* 16:627-638.
- WON, I. J. AND K. SMITS. 1986. Application of airborne electromagnetic methods for bathymetric charting in shallow oceans. In G. I. Palacky, (ed.), *Airborne Resistivity Mapping, Geological Survey of Canada Paper* 82-22:99-104.
- ZIMMERMAN, J. F. T. 1986. The tidal whirlpool: A review of horizontal dispersion by tidal and residual currents. *Netherlands Journal of Sea Research* 20:113-154.

Received for consideration, September 7, 1994
Accepted for publication, June 28, 1996